HUMAN BIOLOGY
2024, VOL. 94, ISSUE 6
ORIGINAL ARTICLE

OPEN ACCESS

Differentially Expressed Genes and Cerna Network of Early Subperiosteal Osteogenesis in Rabbit Skull Defect Models

*Wenxue Wang[1,2], Baodong Zhao[1], Hao Xu[1], Li Zhen[1], Xin Li[1]**

ABSTRACT

Objective: To explore potential critical genes and identify ceRNA network participating in early stage of subperiosteal osteogenesis.

Materials and Methods: Rabbit skull defect models were constructed. The periosteum of defects and control site were obtained 3 weeks postsurgery, and a bioinformatics method was used to analyze differentially expressed (DE) genes and construct a ceRNA regulatory network.

Results: In total, 332 lncRNAs, 22 circRNAs, 37 miRNAs and 1141 mRNAs were differentially expressed. The functional enrichment suggested the immune response, cell-cell interaction, cell proliferation and differentiation, and angiogenesis were associated with wound healing and osteogenesis at an earlier stage. CeRNA networks with 39 lncRNA/ 33 miRNAs/ 51mRNAs and 8 circRNAs/ 9 miRNAs/ 46 mRNAs. were constructed respetively.

Conclusion: Expression gene profiles were significantly altered in periosteum during early healing stages of bone regeneration. This study revealed potentially important genes, pathways and ceRNA regulatory networks participating in intramembranous osteogenesis.

INTRODUCTION

Implant dentures have gradually become an important repair method for dentition defect due to their unique advantages such as comfort, no damage to adjacent teeth, and strong chewing power. The stability of the implant is directly proportional to the degree of osteointegration, which ensures long-term stable function. However, jaw bone atrophy and defects are difficult to treat and have uncertain osteogenic effects, which are currently one of the urgent problems to be solved in clinical practice. How to solve the problems of bone deficiency and bone defects in the implant area, promote bone regeneration, and ensure high-quality and sufficient bone around the implant is a hotspot in the field of oral implantation. Therefore, exploring the molecular mechanisms of endogenous bone growth and identifying potential targets for regulating bone growth is a new approach to solving this problem.

In the 19th century, de Mourgues de Mourgues et al. (1979). discovered that transplanted periosteal tissue can induce new bone growth. The importance of periosteum in bone healing and its extraordinary regenerative ability were first mentioned. Periosteum consists of a double-layer membrane structure. The outer layer is composed of dense collagen fibers, fibroblasts, and their progenitor cells Lin et al. (2014); The internal formation layer contains a large number of periosteum derived progenitor cells (PDPCs) and osteoblasts Yu et al. (2010), both of which jointly initiate and drive the bone repair process, playing a major role in bone remodeling and fracture healing Evans et al. (2013). Recent studies on the regeneration potential of periosteum have shown that compared with cell sources such as bone marrow, periosteum has a higher endogenous regeneration potential and plays an important role in bone repair and regeneration Colnot et al. (2012), Xiao et al. (2020). Therefore, it is of great significance to explore and optimize the factors that regulate osteogenesis of periosteal progenitor cells.

Periosteum plays an important role in enhancing bone formation during dental surgery and maxillofacial reconstruction Taba et al. (2005). There is a lack of data on the exact role of periosteum in bone regeneration and the mechanisms involved. Exploring the molecular events that initiate these behaviors helps to gain a deeper

[1]Department of Oral Implantology, the Affiliated Hospital of Qingdao University, Qingdao 266000, Shandong Province, China.
[2]School of Stomatology of Qingdao University, Qingdao 266000, Shandong Province, China.

Correspondence to: Xin Li, Department of Oral Implantology, the Affiliated Hospital of No. 59 Haier Road, Laoshan District, Qingdao, Shandong Province, China.

Email: lixindentist@126.com, Tel: (0532)82913583.

Keywords: early subperiosteal osteogenesis ; differentially expressed genes ; competing endogenous RNA; functional enrichment.

understanding of endogenous periosteal regeneration and provides information for optimizing tissue engineering construction. However, the gene regulatory network of subperiosteal osteogenesis is still not very clear.

The use of comprehensive sequencing technology for transcriptome analysis is an effective method for characterizing a wide range of biological processes and specific genes expressed in specific cell populations Slovin et al. (2021). Accurate analysis of gene expression profiles in the periosteum can provide a deeper and more detailed understanding in potential osteogenic mechanism. In addition, further exploration of the cellular epigenetic mechanisms related to ceRNA is needed to identify the regulatory targets.

In this study, high-throughput RNA sequencing (RNA-Seq) experiments were conducted to investigate gene expression involved in bone regeneration of periosteum-preserving segmental skull defect in rabbit models. A series of analysis based on the results were performed to explore preliminarily the ceRNA regulatory network and protein network that regulate early response and subsequent subperiosteal osteogenesis.

METHODS

Preparation of rabbit skull defect models

Eight male New Zealand white rabbits aged 3 months were selected. For each animal, the left side of the skull was selected as experimental group, and the right side was left untreated as control group. The subcutaneous tissue was cut under general anesthesia, the periosteum was peeled off intactly and the skull was exposed. Under sufficient cooling of physiological saline, a half layer skull defect with a diameter of 6mm and a depth of 1.5mm was prepared using a drill perpendicular to the skull surface. After complete hemostasis, the periosteum was preserved to cover the bone defect area, intermittent suturing was performed, and the surgical incision was tightly closed.

Periosteal samples collecting

Three weeks after surgery, the periosteum on both sides of the rabbit skull was obtained. Routine disinfection was conducted under general anesthesia, sterile treatment towel was spread to avoid contamination. The skin was opened and the periosteum was exposed. Volume of about 1cm3 periosteal tissue was cut off on both sides, and frozened immediately in liquid nitrogen for 30 seconds, and then the frozen tissues were put it into sterile tubes in different groups. Four samples were taken from experimental group (B) and three samples were taken from control group (A).

High-throughput RNA sequencing (RNA-Seq)

Total RNA was isolated using the Trizol Reagent (Invitrogen, CA, USA). Epicenter Ribo Zero ™ RRNA Removal Kit (Human/Mouse/Lat) was used to exclude ribosomal RNA from total RNA and the RNA was randomly interrupted using divalent cations through ion disruption subsequently.

Using RNA as a template and random oligonucleotides as primers, the first and second strands of cDNA were synthesized. To select cDNA fragments of the preferred 400-500 bp in length, the library fragments were purified using the AMPure XP system (Beckman Coulter, Beverly, CA, USA). PCR amplification was used to enrich the library fragments. Products were purified (AMPure XP system) and quantified using the Agilent high sensitivity DNA assay on a Bioanalyzer 2100 system (Agilent). The sequencing library was then sequenced on NovaSeq 6000 platform (Illumina) by Shanghai Personal Biotechnology Cp. Ltd.

The quality information of raw data in FASTQ format was calculated and then the raw data was filtered using fastp (0.22.0) software. All the subsequent analysis was based on high quality clean data. The reference genome and gene annotation files were downloaded from genome website. The filtered reads were mapping to the reference genome using HISAT2 v2.0.5. The alignment region distribution of mapped reads was calculated.

Differential expression analysis and hierarchical clustering

The differential expression of genes was analyzed by DESeq (v1.38.3) with screened conditions as follows: expression difference multiple $|\log2FoldChange| > 1$, significant P-value < 0.05. Volcano maps of differentially expressed RNAs (mRNA, lncRNA, circRNA, miRNA) were generated using the ggplots 2 R package. R language Pheatmap (v1.0.12) software package was applied to perform bi-directional clustering analysis of RNA tendencies and expression levels of the same gene in different samples and to compare expression patterns of different genes in the same sample.

GO and KEGG enrichment analysis

Gene ontology (GO, http://geneontology.org/) and Kyoto Encyclopedia of Genes and Genomes (KEGG, http://www.kegg.jp/) enrichment analysis were performed on the differentially expressed. target genes. Enriched biological functions including biological processes (BPs), cellular components (CCs), molecular functions (MFs) and KEGG pathways were used to analyze the target DEGs of the ceRNA network. A P value <0.05 was defined as statistically significant.

Target predictions and constructing the ceRNA regulatory network

LncRNA can directly bind to the target gene, it can also interact with miRNA as a ceRNA (competitive endogenous RNA), and participate in the regulation of

target gene expression. CircRNA can adsorb miRNAs and inhibit the function of miRNAs. Based on this significant theory, MiRanda (v3.3a) software were used to predict miRNA target genes. A ceRNA regulatory network of lncRNA-miRNA-mRNA and circRNA-miRNA-mRNA was thus constructed to explore the regulatory relationship in Cytoscape version 3.6.1.

Protein-protein interaction (PPI) analysis

A PPI network was constructed by the Search Tool for the Retrieval of Interacting Genes/Proteins (STRING), Based on the results of differentially expressed genes, the PPI effect was screened in the database for nodes with both ends being differentially expressed genes and a score>0.95.

RESULTS

General observation 3-week post-surgery

Three weeks after surgery, all wounds of rabbits were not infected and sutures were not loose. Bone defects were found to be completely healed after incision and flaping, and periosteum corresponding to bone defects was thickened.

PCA analysis

PCA analysis can gather similar samples together, and the closer the distance, the higher the similarity between samples. As shown in Figure.1, the results showed that each sample in different groups (4 in the experimental group and 3 in the control group) had biological replicability parallelism, and there were inter group differences between the experimental and the control group, which proved that the sampling was reasonable and the results of subsequent difference analysis were consistent with biostatistical principles.

Figure 1: PCA analysis of different groups. The horizontal axis represents the first principal component, and the vertical represents the second principal component. Different shapes in the figure represent different samples, and the different colors represent different groups. Condition A refers to control groups and B refers to the experimental groups.

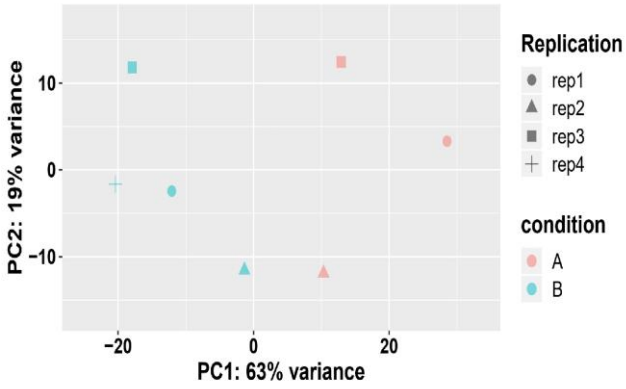

Expression difference analysis

Transcriptome analysis results were showed in table 1, in experimental group, there are 332 significant lncRNAs (106 upregulated and 226 downregulated), 22 significant circRNAs (10 upregulated and 12 downregulated), 37 significant miRNAs (24 upregulated and 13 downregulated) and 1141 significant mRNAs (439 upregulated and 709 downregulated) in comparison with control group. In addition, differential expressed genes were identified by a heatmap Figure. 2A and Volcano plot, respectively Figure. 2B.

Table 1: Expression difference analysis of RNAs

	Up-regulated	Down-regulated	Total
mRNAs	432	709	1141
lncRNAs	106	226	332
circRNAs	10	12	22
miRNAs	24	13	37

Functional enrichment analysis of differentially expressed genes

GO enrichment analysis

The GO enrichment analysis results of differentially up-expressed genes were classified according to molecular function MF, biological process BP, and cellular component CC. The top 10 GO terms with the smallest p-value or the most significant enrichment were selected from each GO classification for display. The results are shown in Figure 3. The cell components involved were mainly cell periphery, lytic vacuole, late endosome ect.; molecular function mainly involved hydrolase activity, G-protein alpha-subunit binding, carbohydrate binding, cytokine receptor activity, immune function; Biological processes are mainly focused on immune response and response to external stimulus.

KEGG enrichment analysis

Based on the KEGG enrichment analysis of differentially up-expressed genes, the top 30 pathways with the smallest

Figure 2: Identification of the significant expression changes of RNAs

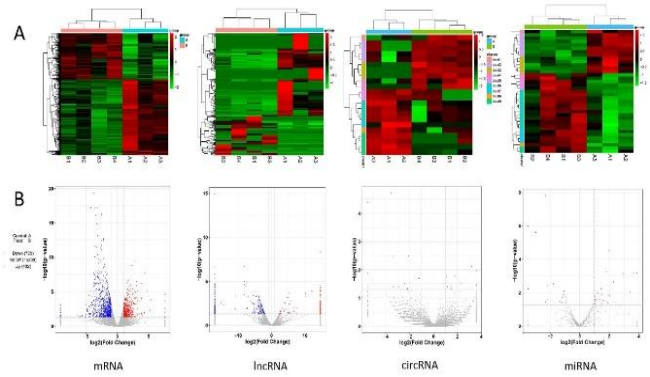

(A) heatmap: Genes are represented horizontally, each column represents a sample, with red representing highly expressed genes and green representing low-expressed genes.

(B)Volcano map: The red dots represent upregulated genes in this group, the blue dots represent downregulated genes, and the gray dots represent non-significantly differentially expressed genes.

Figure 3: GO enrichment analysis

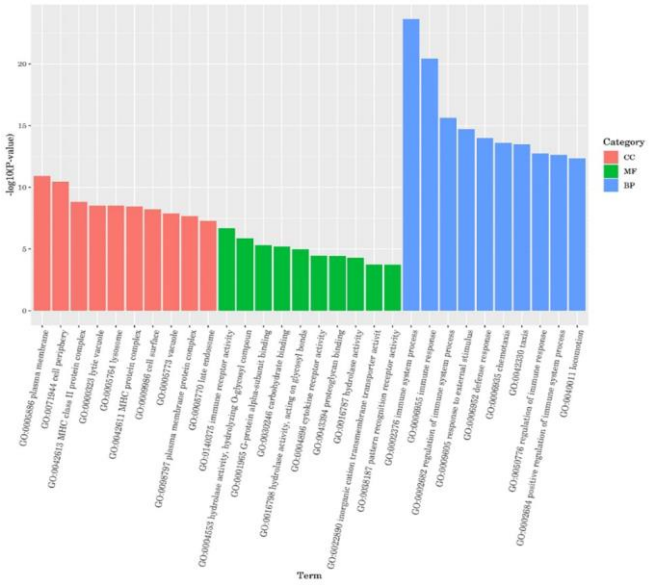

p-value and the most significant enrichment were selected for display. The results are shown in table 2. Among these pathways, 15 belong to the level of immune system and are consistent with GO analysis. The other pathways are related to cell metabolism, cell proliferation and differentiation, and angiogenesis.

Protein-protein interaction (PPI) analysis

The interrelationships between proteins were shown in figure 4. The nodes in this figure represented genes or proteins, and if there are lines between the two nodes, it means that there is a protein interaction between the two genes or proteins. There were 214 pairs of genes in the PPI network.

Figure 4: PPI analysis. Green nodes represent down-regulated mRNAs or proteins, and the red represent up-expressed mRNAs or proteins.

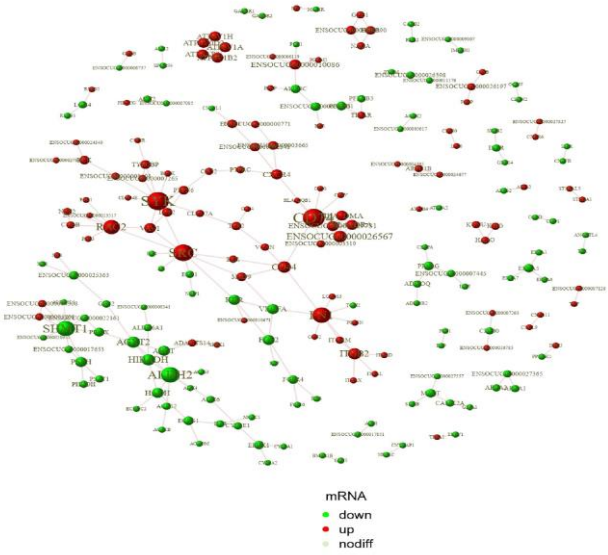

Construction of the ceRNA regulatory Network

The screening sensitivity correlation was set>0.3, and 39 DElncRNA were able to target 33 DEmiRNAs, these DEmiRNAs may bind to 51 DEmRNAs.

Four circRNAs were able to target 9 DEmiRNAs which may bind to 6 DEmRNAs. a ceRNA network of circRNA-miRNA-mRNA (Figure 5A) and lncRNA-miRNA-mRNA (Figure 5B) was constructed and presented through Cytoscape.

Figure 5: A. CircRNA-miRNA-mRNA network. Red nodes represent mRNAs, green represent circRNAs, and the lines connecting them indicate miRNAs.

B. LncRNA-miRNA-mRNA network. Red nodes represent mRNAs, green represent lncRNAs, and the lines connecting them indicate miRNAs.

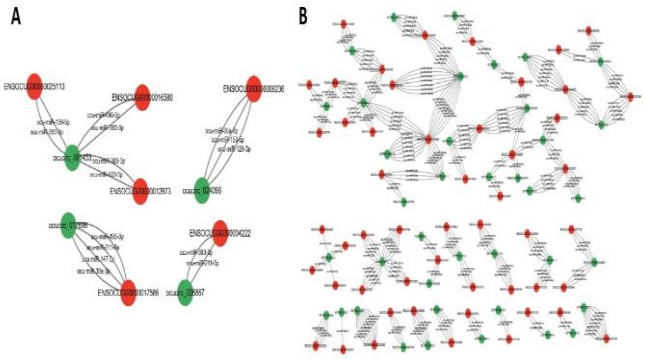

Table 2: KEGG enrichment analysis of top 30

Pathway	Level2	Pvalue	FDR
Lysosome	Transport and catabolism	5.30E-15	1.27E-12
Phagosome	Transport and catabolism	7.56E-10	4.52E-08
Other glycan degradation	Glycan biosynthesis and metabolism	2.02E-07	9.65E-06
Cell adhesion molecules	Signaling molecules and interaction	7.73E-07	2.64E-05
Hematopoietic cell lineage	Immune system	2.92E-06	8.71E-05
Natural killer cell mediated cytotoxicity	Immune system	3.96E-06	9.46E-05
Toll-like receptor signaling pathway	Immune system	6.26E-06	0.000136012
Fc gamma R-mediated phagocytosis	Immune system	7.23E-06	0.00014404
Chemokine signaling pathway	Immune system	8.29E-06	0.000152377
Glycosphingolipid biosynthesis - ganglio series	Glycan biosynthesis and metabolism	1.68E-05	0.000268408
Neutrophil extracellular trap formation	Immune system	3.19E-05	0.000475938
Regulation of actin cytoskeleton	Cell motility	4.39E-05	0.000616979
C-type lectin receptor signaling pathway	Immune system	5.76E-05	0.000724724
B cell receptor signaling pathway	Immune system	6.31E-05	0.000754581
Osteoclast differentiation	Development and regeneration	0.000143179	0.001487814
Glycosphingolipid biosynthesis - globo and isoglobo series	Glycan biosynthesis and metabolism	0.000236104	0.002257156
Glycosaminoglycan degradation	Glycan biosynthesis and metabolism	0.000887089	0.007571935
Leukocyte transendothelial migration	Immune system	0.003930041	0.02538594
Cytokine-cytokine receptor interaction	Signaling molecules and interaction	0.005213594	0.031949971
Galactose metabolism	Carbohydrate metabolism	0.005569877	0.032468307
T cell receptor signaling pathway	Immune system	0.008825822	0.048077306
Complement and coagulation cascades	Immune system	0.008851052	0.048077306
Glycolysis / Gluconeogenesis	Carbohydrate metabolism	0.013738363	0.069861036
Fc epsilon RI signaling pathway	Immune system	0.013738363	0.069861036
Endocytosis	Transport and catabolism	0.021557087	0.09873185
Rap1 signaling pathway	Signal transduction	0.021588081	0.09873185
Phospholipase D signaling pathway	Signal transduction	0.021894511	0.09873185
Collecting duct acid secretion	Excretory system	0.028271952	0.122078175
Synaptic vesicle cycle	Nervous system	0.031417084	0.129579826
Amino sugar and nucleotide sugar metabolism	Carbohydrate metabolism	0.035562763	0.14165834
VEGF signaling pathway	Signal transduction	0.035562763	0.14165834
Calcium signaling pathway	Signal transduction	0.037397747	0.146525601
Platelet activation	Immune system	0.047253317	0.173746813
Apoptosis	Cell growth and death	0.048786774	0.174754894
Focal adhesion	Cellular community - eukaryotes	0.058565092	0.191740509
PI3K-Akt signaling pathway	Signal transduction	0.058565093	0.191740509
NF-kappa B signaling pathway	Signal transduction	0.08226589	0.252071125

DISCUSSION

Although the regenerative ability of the periosteum has been demonstrated, its application as a regenerative tool is seriously underestimated, especially in the field of oral and maxillofacial surgery Mahajan et al. (2012). Notably, periosteum meets the three main conditions for tissue engineering: cells, scaffolds for cell maintenance and delivery, and local growth factors. However, little is known about the precise role of periosteum and mechanism of periosteal-mediated bone regeneration. Therefore, study on osteogenic molecular regulation mechanisms has certain enlightening significance for mandibular defects reconstruction and guided bone generation around implants.

The emergence of high-throughput sequencing provides reliable assurance for identifying potential critical biomarkers. The regulatory network of lncRNAs /miRNAs /mRNAs and circRNAs /miRNAs /mRNAs at periosteum tissues could be, therefore, investigated via bioinformatics analyses Xu et al. (2021). The results in this study demonstrated that a variety of novel genes and pathways (including KEGG pathway and ceRNA network) are possibly involved in periosteum-mediated osteogenesis.

Bone regeneration involves four consecutive stages and is a complex and comprehensive process. These four stages include the initial inflammatory response and recruitment of bone progenitor cells, formation of cartilage callus tissue, replacement of cartilage with sponge bone, and finally the remodeling of immature bone towards mature lamellar bone. The periosteum is the main contributor to the complex processes that run through all these stages Colnot et al. (2009), Zhang et al. (2005).

When the defect occurs, the inflammatory cascade is initiated to activate inflammatory cells near the defect, which further secrete growth factors and recruit cells with bone repair ability to start the defect repair Bahney et al. (2019). Macrophages recruit periosteal cells by secreting platelet-derived growth factor-BB (PDGF-BB) Gao et al. (2019). PDGF-BB and its receptors mediates the proliferation of periosteal cells in the initial stage through PDGFRβ-PI3K signal axis, and promote their rapid involvement in defect repair Doherty et al. (2019).

GO enrichment of up-expressed genes in this study showed that in terms of biological processes (BP), early periosteal mediated bone regeneration was associated with enhanced inflammation and immune responses. Pathways such as chemokine signaling pathway, NF-kappa B signaling pathway and platelet activation in KEGG analysis also suggests the early inflammatory stage of bone regeneration. The cellular inflammatory and immune response may lead to improved bone regeneration outcomes and these results are in agreement with an immature healing wound.

After injury, periostin is secreted by periosteum cells to participate in defect repair by regulating cell-cell and cell-matrix interactions. The periosteal cells that migrated to the defect site can differentiate into osteoblasts and chondroblasts under the regulation of Wnt/β-catenin, TGF/BMP, PI3K-Akt and other signaling pathways Kegelman et al. (2021). Intramembranous osteogenesis and intrachondral osteogenesis were used to repair the defect. In this study, the cellular component (CC) in GO analysis were mainly concentrated on cell periphery, plasma membrane, plasma membrane protein complex, revealing the interaction between cells, and indicating early osteogenesis events; VEGF signaling pathway, PI3K-Akt signaling pathway, ECM-receptor interaction, TNF signaling pathway in KEGG analysis indicates that the cells have been recruited to the defect area and the osteogenesis process has begun. Based on the functional enrichment analysis, it is believed that the time point is a critical early bone regeneration period, and the results of transcriptional profiles, ceRNAs and relevant signal pathways in this study could provide better analysis for molecular mechanisms of periosteum during early stage of bone regeneration.

MicroRNAs (miRs) are small, non-coding RNAs that act as important post transcriptional regulators of gene expression by inhibiting mRNA translation or inducing mRNA degradation. MiRs play a crucial regulatory role in bone formation, bone remodeling, and bone degradation Hensley et al. (2021), Giordano et al. (2020), Oliviero et al. (2019). By targeting multiple proteins and signal pathways, miRs regulate each differentiation step and exert positive or negative effects on osteogenesis Gargano et al. (2021), Taipaleenmäki et al. (2018), Gargano et al. (2022). In this study, there are 13 down-regulated miRNAs (such as miR-708-3p, miR-153-3p, miR-129-5p, miR-30a-3p), most of which has negative effect on osteogenesis. Scholars have demonstrated that miR-153-3p can inhibits osteogenic differentiation of periodontal ligament stem cells Jiang et al. (2021). In addition, miR-708-3p was reported to be highly expressed in osteoporosis patients and regulate osteoclast differentiation positively in bone marrow monocytes Wang et al. (2020). MiR-30a-3p was found to promote ovariectomy-induced osteoporosis in rats via targeting SFRP Liu et al. (20419). Studies have shown that RNAs with MERs (miRNA reaction elements) regulate each other, and this regulatory mechanism is called the ceRNA hypothesis (Competing endogenous RNAs). LncRNA and circ RNA act as ceRNA, and reduce the expression of miRNA through MERs, thereby trimming down the inhibitory effect of corresponding miRNA on other target genes. For transcripts such as lncRNA, mRNA, and circRNA, they may compete with each other for miRNA binding, forming a ceRNA regulatory network. The stability of ceRNA networks is of great significance for maintaining normal biological functions. LncRNAs and circRNAs play an essential regulatory role in disease

through interactions with disease-related miRNAs, and have been shown to be epigenetic regulators with significant involvement in bone metabolism Yang et al. (2020), Gargano et al. (2023). Therefore, the prediction of miRNA target genes in newly identified lncRNAs and circRNAs will facilitate further function investigation. In this study, 4 significant DEcircRNAs and 39 DElncRNAs from the results of an RNA-Seq experiment possessed miRNA binding sites in the ceRNA network, and some of them presented an opposite trend in expression of miRNAs which participate in metabolism of bone tissue. Therefore, we speculated that these ceRNAs have a potential function of specifically interaction with miRs to regulate the expression of downstream genes in osteogenesis.

CONCLUSION

The findings of this study revealed potentially important genes, pathways, and ceRNA regulatory networks associated with bone modeling and metabolism. These findings hold significant implications for understanding the potential mechanisms of subperiosteal osteogenesis in jawbones. However, more comprehensive analyses and further in-depth studies, including in vitro and in vivo experiments, are still required to fully investigate these associations.

DECLARATIONS

Author contributions

Wenxue Wang: Conduct the experiment, collect the data, writing original draft. Baodong Zhao: Analyze the data. Hao Xu: Methodology. Li Zhen: Conduct some part of the experiment. Xin Li: project administration, conducting experiment, methodology, writing—review and editing.

Fundings

Medical and Health Science and Technology Development Project of Shandong Province [Project NO 202208050566], the Natural Science Foundation of Qingdao Municipality [Project 23-2-1-133-zyyd-jch] and Natural Science Foundation of Qingdao University.

Ethics approval and consent to participate

The study design and protocol were approved by the Ethics Committee of Affiliated Hospital of Qingdao University (QDFYWZLL28384). In this study, we adhered to the Declaration of Helsinki (2013). The all methods meet the requirements of moral, ethical and scientific principles.

Availability of data and materials

The transcriptome clean raw reads data used and analysed during the current study available from the corresponding author on reasonable request. The authors have to declare that they embedded all data in the manuscript.

Consent for publication

Not applicable.

Competing interests

This study does not have conflict of interest with any individual or institution.

REFERENCES

1. de Mourgues G. Léopold Ollier. 1979. the father of orthopedic surgery. Rev Chir Orthop Reparatrice Appar Mot. 65 Suppl 2:2-3.

2. Lin Z, Fateh A, Salem DM. et al. 2014. Periosteum: biology and applications in craniofacial bone regeneration. J Dent Res. 93:109–16.

3. Yu YY, Lieu S, Lu C. et al. 2010. Bone morphogenetic protein 2 stimulates endochondral ossification by regulating periosteal cell fate during bone repair. Bone. 47:65–73.

4. Evans SF, Chang H, Knothe Tate ML. 2013. Elucidating multiscale periosteal mechanobiology: a key to unlocking the smart properties and regenerative capacity of the periosteum? Tissue Eng Part B Rev. 19:147-59.

5. Colnot C, Zhang X, Knothe Tate ML. 2012. Current insights on the regenerative potential of the periosteum: molecular, cellular, and endogenous engineering approaches. J Orthop Res. 30:1869–78.

6. Xiao H, Wang L, Zhang T. et al. 2020. Periosteum progenitors could stimulate bone regeneration in aged murine bone defect model. J Cell Mol Med. 24:12199–210.

7. Taba M, Jin Q, Sugai JV, et al. 2005. Current concepts in periodontal bioengineering. Orthod Craniofac Res. 8:292-02.

8. Slovin S, Carissimo A, Panariello F, et al. 2021. Single-Cell RNA Sequencing Analysis: A Step-by-Step Overview. Methods Mol Biol. 2284:343-65.

9. Mahajan A. 2012. Periosteum: a highly underrated tool in dentistry. Int J Dent. 2012:717816.

10. Xu SL, Deng YS, Liu J, et al. 2021. Regulation of circular RNAs act as ceRNA in a hypoxic pulmonary hypertension rat model. Genomics. 113:11-19.

11. Colnot C. 2009. Skeletal cell fate decisions within periosteum and bone marrow during bone regeneration. J Bone Miner Res. 24(2):274-82.

12. Zhang X, Xie C, Lin AS, et al. 2005. Periosteal progenitor cell fate in segmental cortical bone graft

transplantations: implications for functional tissue engineering. J Bone Miner Res. 20:2124-37.

13. Bahney CS, Zondervan RL, Allison P, et al. 2019. Cellular biology of fracture healing. J Orthop Res. 37:35-50.

14. Gao B, Deng R, Chai Y, et al. 2019. Macrophage-lineage TRAP+ cells recruit periosteum-derived cells for periosteal osteogenesis and regeneration. J Clin Invest. 129(6): 2578-94.

15. Doherty L, Yu J, Wang X, et al. 2019. A PDGFRβ-PI3K signaling axis mediates periosteal cell activation during fracture healing. PLoS One. 14:e0223846.

16. Kegelman CD, Nijsure MP, Moharrer Y, et al. 2021. YAP and TAZ Promote Periosteal Osteoblast Precursor Expansion and Differentiation for Fracture Repair. J Bone Miner Res. 36(1):143-57.

17. Hensley AP, McAlinden A. 2021. The role of microRNAs in bone development. Bone. 143:115760.

18. Giordano L, Porta GD, Peretti GM, et al. 2020. Therapeutic potential of microRNA in tendon injuries. Br Med Bull. 133:79-94.

19. Oliviero A, Della Porta G, Peretti GM, et al. 2019. MicroRNA in osteoarthritis: physiopathology, diagnosis and therapeutic challenge. Br Med Bull. 130:137-47.

20. Gargano G, Oliviero A, Oliva F, et al. 2021. Small interfering RNAs in tendon homeostasis. Br Med Bull. 138:58-67.

21. Taipaleenmäki H. 2018. Regulation of Bone Metabolism by microRNAs. Curr Osteoporos Rep. 16:1-12.

22. Gargano G, Oliva F, Oliviero A, et al. 2022. Small interfering RNAs in the management of human rheumatoid arthritis. Br Med Bull. 142:34-43.

23. Jiang H, Jia P. 2021. MiR-153-3p inhibits osteogenic differentiation of periodontal ligament stem cells through KDM6A-induced demethylation of H3K27me3. J Periodontal Res. 56:379-87.

24. Wang R, Feng Y, Xu H, et al. 2020. Synergistic effects of miR-708-5p and miR-708-3p accelerate the progression of osteoporosis. J Int Med Res. 48:300060520978015.

25. Liu HP, Hao DJ, Wang XD, et al. 2019. MiR-30a-3p promotes ovariectomy-induced osteoporosis in rats via targeting SFRP1. Eur Rev Med Pharmacol Sci. 23:9754-60.

26. Yang Y, Yujiao W, Fang W, et al. 2020. The roles of miRNA, lncRNA and circRNA in the development of osteoporosis. Biol Res. 53:40.

27. Gargano G, Asparago G, Spiezia F, et al. 2023. Small interfering RNAs in the management of human osteoporosis. Br Med Bull. 148:58-69.

